Thermal Analysis of a Canned Induction Motor for Main Coolant Pump in System-Integrated Modular Advanced Reactor

Hyung Huh*, Jong-In Kim* and Kern-Jung Kim**

Abstract - The three-phase canned induction motor, which consists of a stator and rotor with a seal can, is used for the main coolant pump (MCP) of the System-integrated Modular Advanced Reactor (SMART). The thermal characteristics of the can must be estimated exactly, since the eddy current loss of the can is a dominant parameter in design. Besides the insulation of the motor winding is compared of Teflon, glass fiber, and air, so it is not an easy task to analyze. A FEM thermal analysis was performed by using the thermal properties of complex insulation which were obtained by comparing the results of finite element thermal analysis and those of the experiment. As a result, it is shown that the characteristics of prototype canned induction motor have a good agreement with the results of FEM.

Keywords: three-phase canned induction motor, thermal analysis, SMART MCP, FEM

1. Introduction

The SMART (System–Integrated Modular Advance Reactor) MCP (Main Coolant Pump) is a canned motor pump that requires no pump seals. This characteristic basically eliminates a small break a loss of coolant accident, which is associated with the pump seal failure, and this characteristics becomes a basis of conventional pump design. SMART has four MCPs vertically installed on the top annular cover of the Reactor Pressure Vessel. Each is an integral unit consisting of a canned asynchronous three- phase induction motor and an axial-flow single-stage pump. The motor rotor and the impeller shaft are connected by a common shaft rotating on two radial and one axial thrust bearings, which use a specialized graphite-based material.

Cooling of the motor is accomplished with the component cooling water, which flows through the tubes wound helically along the outer surface of motor stator. Since the material of the can is a conductor, the eddy current generates a lot of heat is in the can This heat causes the temperature of the water, which is flowing into the air gap for bearing, to continue to rise. An external cooling system cools the water for the bearing lubrication. In this study, we clarified the temperature characteristics of the canned motor for the MCP vis experiments and simulation, and verified the propriety of the method for thermal analysis by comparing it with the results.

2. Specification

The MCP cooling system is composed of cooling water flowing in the motor air-gap by using an independent circuit. In other words on the outside wall of the stator core, cooling water is provided by the external cooling loop. The cooling water temperature of the independent circuit rises due to the eddy current in the can and the high temperature water flows to the outside of the stator core. The water then flows between the external circuit cooling tubes as shown in Fig. 1. Therefore, the temperature of the water decreases due to heat exchange with external circuit cooling water.
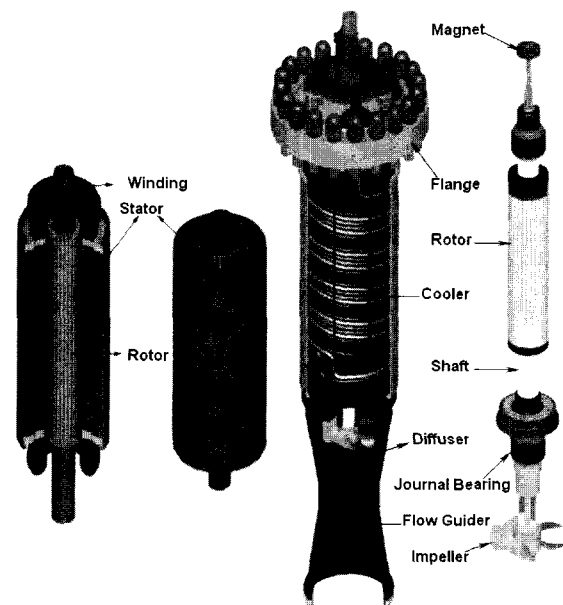

Fig. 1 Main coolant pump and canned motor

* Div. of Mechanical Engineering, Korea Atomic Energy Research Institute, Korea. Hyung Huh can be reached at hhuh@kaeri.re.kr.
** Dept. of Electrical Engineering, ChungNam National Univerity, Korea and can be reached at kjkim@ee.chungnam.ac.kr.

This water flows into the air-gap again and the temperature of the external circuit cooling water rises via heat exchange with the independent circuit cooling water, and the water returns to the main system. The cooling effect in the concerned motor is generated by the repetition of this process. Since the MCP must be operated in two modes, low speed and normal speed, the MCP is driven by a Variable Voltage Variable Frequency (VVVF) inverter. The MCP is operated at 900 rpm as the frequency of the inverter is 15Hz in the low speed mode, and it is operated at 3,600 rpm as the frequency of inverter is 60Hz in normal speed mode[1].

The thickness of the stator can and the rotor can are 0.5mm and 0.6mm respectively, and both are made of stainless steel, which can endure the internal high pressure of the MCP and reduce the eddy current[2].

Table 1 shows the design specification of the motor.

3. Heat Transfer

The heat generated by the motor is the same as the sum of the heat eliminated by the convection that occurs from the flow of the independent circuit cooling water and the heat discharged to the atmosphere from the motor surface. The temperature of the motor increases, and after a certain time, the temperature remains constant, reaching a steady state. The heat equation is defined in Equation (1) and the equation of energy conservation for the surface occurring convection heat transfer is shown in Equation (2) [3], [4].

$$\frac{1}{r}\frac{\partial}{\partial r}\left(kr\frac{\partial T}{\partial r}\right)+\frac{1}{r^2}\frac{\partial}{\partial\phi}\left(k\frac{\partial T}{\partial\phi}\right)+\frac{\partial}{\partial z}\left(k\frac{\partial T}{\partial z}\right)+q=\rho c_{\mathrm{p}}\frac{\partial T}{\partial t} \quad (1)$$

$$E_{\mathrm{g}}-hA(T_{\mathrm{s}}-T_{\infty})=\rho c_{\mathrm{p}}V\frac{\partial T}{\partial t} \quad (2)$$

where r is the radius, k is thermal conductivity, T is temperature, ϕ is an azimuthal angle, q is the rate of energy
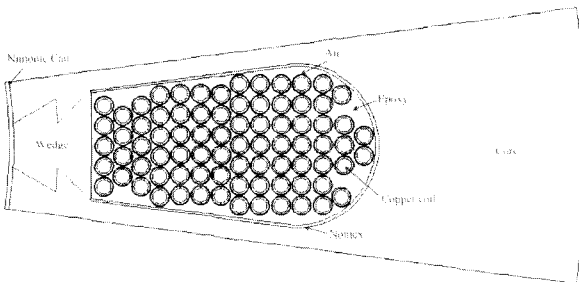

Fig. 2 Model for thermal analysis

Table 1 Design specification of the canned motor

Items		Value
Output Power		32kW
Number of Pole		2
Frequency	Low Speed Mode	15Hz
	Normal Speed Mode	60Hz
Voltage		400V
Core Length		430mm
Stator	Outside Diameter	240mm
	Inside Diameter	110mm
Rotor	Outside Diameter	105mm
Number of Slot	Stator	24
	Rotor	28
Air-gap	Mechanical	1.4mm
	Effective	2.5mm

generation per unit volume, ρ is mass density, c_p is specific heat, V is volume, E_g is the rate of energy generation, h is convection heat transfer coefficient, and subscript s is surface and subscript ∞ is ambient. T_∞ and h of Equation (2) are decided by thermal and fluid properties of the independent circuit cooling water in the stator [5].

$$Nu = f(\mathrm{Re}, \mathrm{Pr}) \quad (3a)$$

$$h = f(Nu, d, k) \quad (3b)$$

$$Re = \frac{\rho v d}{\mu} \quad (4)$$

$$Pr = \frac{c_p \mu}{k} \quad (5)$$

$$Nu = \frac{hd}{k} \quad (6)$$

where Re is the Reynolds number, Pr is the Prandtl number and Nu is the Nusselt number

4. Thermal Analysis

4.1 Model of Thermal Analysis

The surface of the conductor is covered with weaved glass-fiber, and then insulated with Teflon and finally im-

pregnated with Epoxy. However, Teflon cannot adhere to Epoxy, so a very thin air-gap exists between them. Therefore, creating a model for analysis that consists of the whole model, considering complex and dense parts, is difficult. In this study, we developed the 2D model to simulate one slot that is 1/24 of the whole model stator, and the actual number of conductors in one slot is 80. In addition, we assumed a 0.1mm air-gap thickness between the Teflon and Epoxy. Since the second insulator, Teflon, is very thin, the analysis model is simulated without Teflon.

4.2 Condition of Thermal Analysis

The analysis condition applied in this study is the same as the experimental condition and the results of the experiment, and the analysis after analyzing temperature characteristics of the motor for MCP. Table 2 shows the experimental condition of the motor that is operated at the rated power. The temperatures are measured at points A, B, C, and D (shown in Fig. 1) with the thermocouples of T-type when the cooling waters have reached the thermal steady state. In this analysis, the losses from windings, the core, and the can of the motor can be decided by the specification and by driving conditions. The losses from windings and from the core can are defined as in Equations (7) and (8).

$$P_{vu} = \rho \int_I J^2 d\mathcal{V}' \; [\text{W}] \tag{7}$$

$$P_v = 4.97 \left(\frac{B_p}{B_0}\right)^{1.942} \left(\frac{f}{f_0}\right)^{1.45} \tag{8}$$

where ρ is the resistivity of windings, J is the current density of windings, B_p is the maximum flux density of core, f is the frequency of flux, and B_0 and f_0 are standard flux density and frequency. The can, which covers the stator teeth part, can be considered as a part of the squirrel cage bar at standstill, and its resistance can be represented as in Equation (9). In addition, the can that does not contact the stator teeth part can be considered the end-ring part of the rotor, and therefore, it is represented as shown in Equation (10). So, the total loss of the can is represented in (11) and the generating loss value of the can is equal to Equation (12) [6].

$$Can_{bar} = \frac{m \times \rho \times (Ck_w)^2 \times L_t}{\mu \times D_t \times Can_t} [\Omega] \tag{9}$$

$$Can_{Ring} = \frac{m \times \rho \times (Ck_w)^2 \times D_t \times 0.637}{(Can_t - L_t) \times Can_t} [\Omega] \tag{10}$$

$$Can_{Re} = Can_{Bar} + Can_{Ring} [\Omega] \tag{11}$$

$$Can_{Loss} = \frac{m \times V^2}{Can_{Re}} [kW] \tag{12}$$

where m is number of phase, ρ is resistivity, C is number of series conducting, k_w is winding factor, L_t is length of stator, D_t is inner diameter of stator, Can_t is length of can, Can_t is thickness of can, and V is the line voltage.

Table 2 Design specification of the canned motor

Items	Value
Output Rated Power	32 kW
Frequency	60 Hz
Speed	3,600 rpm
Voltage	400 V
Current Density	4.5 A/mm^2
External Loop Temp. of Inlet	26 °C
Cooling Water Flow Rate	0.6 m/s

Since the convection heat transfer coefficients on the stator surface is decided by the flow rate of the independent loop cooling water, the flow rate must be accurately determined.

The total loss of the motor during rated operation is approximately 9.5kW and the heat-transfer rate of the external loop cooling water is measured to be 6kW.

Therefore, 3.5kW of the total loss from the motor is the heat released to the atmosphere from the motor surface. Of course, some errors are present, but the heat-transfer rate of the independent loop cooling water is considered to be 6kW by applying the heat balance with the external loop cooling water.

4.3 Results of Analysis

We performed a thermal analysis for the stator of the motor by applying the analysis conditions in Table 3.

The temperature distribution is shown in Fig. 3 and Fig. 4 shows the temperature characteristics of the radial direction.

The maximum temperature of windings in the analysis result is about 75 °C.

Table 3 Analysis input data

Items		Value
Loss	Winding	51.5W
	Can	181W
	Core	27.8W
Thermal Conductivity	Glass-fiber	1.4 W/m°C
	Teflon	0.2 W/m°C

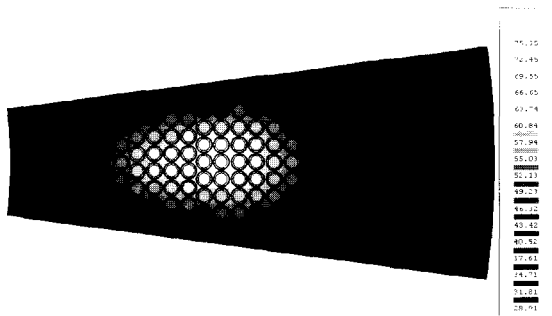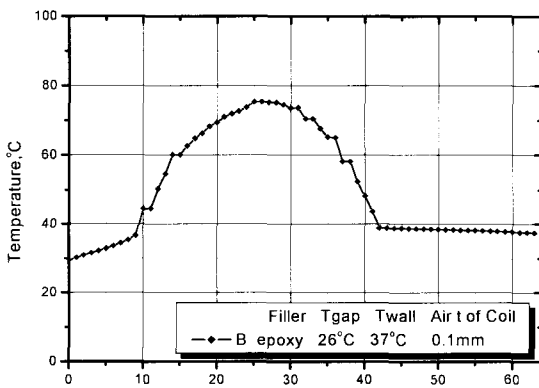|	Nomex	0.105W/m°C
	Epoxy	0.5 W/m°C
	Air	0.0263 W/m°C
	Water	0.6328 W/m°C
Independent Loop Cooling Water	Inlet Temp.	26°C
	Outlet Temp.	37°C
Convection Heat Transfer Coefficient	Inner Stator	9.634 w/m² °C
	Outer Stator	15.112 w/m² °C
Boundary Condition		Neumann Condition/ Convection Surface Condition

Fig. 3 FEM result of the stator coil

Fig. 4 FEM temperature distribution in radial direction of the stator

4.4 Results of Experiment

The temperatures of windings measured at points A, B, C, and D as shown in Fig. 1 are 63℃, 67℃, 74℃, and 127℃, respectively. Table 4 shows the analytical result is 1-12℃ higher than the experimental results. Fig. 5 shows the integrated experimental system of the canned induction motor and Fig. 6 shows the experimental result at each point.

4.5 Thermal Analysis Considering Reactor Operation

The proposed method for the thermal analysis in this study was used for predicting the thermal characteristics of the motors that are actually operating in the nuclear reactor or of which the rated power is different. The detailed

analysis conditions are listed in Table 5. Fig.7 shows temperature characteristics for the radial direction of the stator when output power is 32 kW (rated) and 46 kW (overloaded). As shown in Fig. 7, the maximum winding temperatures of 32 kW and 46 kW are 115°C and 135°C, respectively.

Table 4 Comparison of calculated and measured temperatures of the stator coil

Point	Max. Temp. of Winding		$T_{anal.}-T_{exp.}$
	Analysis	Experiment	
A/①	75 °C	63 °C	-12°C
B/②	75 °C	67 °C	-8°C
C/③	75 °C	74 °C	-1°C
D/④	-	127 °C	-
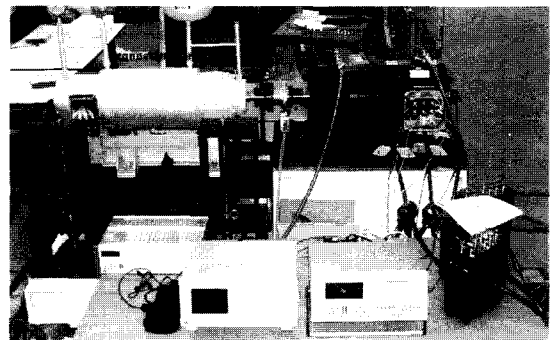
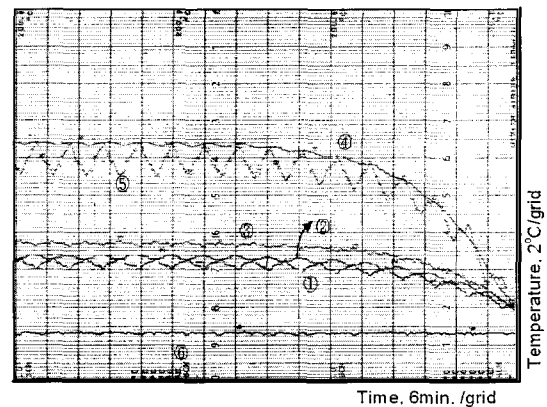**Fig. 5** Experimental system of canned induction motor

Time, 6min. /grid

Fig. 6 Measured temperature of the stator winding

Table 5 Condition of analysis considering MCP operating in the reactor

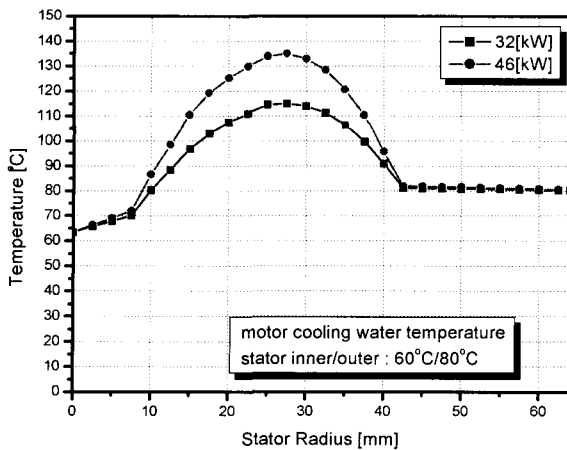| Items		32k W	46 kW
Loss	Winding	51.5 W	106.1 W
	Core	27.8 W	27 W
Temp.of Cooling Water	Inlet Temp.	60 °C	60°C
	Outlet Temp	80 °C	80°C
Convection Heat Transfer Coefficient	Inner Stator	10.682 w/m² °C	
	Outer Stator	15.858 w/m² °C	
Fluid Velocity	Internal	1.76 m/s	
	External	2.65 m/s	

Fig. 7 FEM temperature distribution in radial direction of the stator [indep. circuit cooling water temp. 60°C]

5. Conclusions

The results of the FEM and the experiments in this work lead to the following conclusions.

The analytical average temperature of windings, 75°C, appeared to be 1-12°C higher than the experimental results. Errors appeared to be present between the analytical result and the experimental result because the actual thickness of the air-gap between the Teflon and Epoxy could be thinner than the 0.1 mm used as an input for the thermal analysis. Therefore, a more correct result will be obtained if study continues on the thickness of the air-gap between the Teflon and Epoxy.

The thermal analysis results considering MCP operated in the reactor showed that the maximum winding temperature of the output rated power and overloaded power is within the allowable limit.

An FEM thermal analysis was performed by using the thermal properties of complex insulation which were obtained by comparing the results of the finite element thermal analyses and those of the experiment. These results could be useful for predicting thermal characteristics of the motors when the rated power is different.

Acknowledgements

References

[1] Jang-Hwan Kim, Jong-Woo Choi and Seung-Ki Sul, "New Strategy to Estimate The Rotor Flux of Induction Motor by Analyzing Observer Characteristic Func-

tion.", *KIEE International Transactions on Electrical Machinery and Energy Conversion Systems*, vol. 11B, no. 2, pp. 51-58, June, 2001.

[2] G. Muller and J. Schneider, "High Efficient Induction Motors-The Role of Electrical Steels with Improved Magnetizing Behavior.", *KIEE International Transactions on Electrical Machinery and Energy Conversion Systems*, vol. 11B, no. 3, pp. 75-80, September, 2001.

[3] F.P. Incropera and D.P. Dewitt, *Fundamentals of Heat and Mass Transfer*, John Wiley & Sons, 1996.

[4] J.P. Holman, *Heat Transfer*, McGraw-Hill, 1990.

[5] F.M. White, *Fluid Mechanics*, McGraw–Hill, 1995.

[6] C.G. Veinott, *Theory and Design of Small Induction Motor*, McGraw-Hill, 1994.

Hyung Huh
He is currently working toward the Ph.D. degree at the ChungNam National University. His research interests are motor and sensor design, and NDT.

Jong-In Kim
He received the Ph.D. in Mechanical Engineering from ENSM University. in France. His research interests are nuclear power plant equipment design and development.

Kern-Jung Kim
He received the Ph.D. degree in Electrical Engineering from Seoul National University. His research interests are power system stability and planning.